Inorganic Chemistry

Article

pubs.acs.org/IC

Theoretical Study on the Transition-Metal Oxoboryl Complex: M−BO Bonding Nature, Mechanism of the Formation Reaction, and Prediction of a New Oxoboryl Complex

Guixiang Zeng and Shigeyoshi Sakaki*

Fukui Institute for Fundamental Chemistry, Kyoto University, Takano-Nishihiraki-cho 34-4, Sakyo-ku, Kyoto 606-8103, Japan

Supporting Information

ABSTRACT: The Pt−BO bonding nature and the formation reaction of the experimentally reported platinum(II) oxoboryl complex, simplified to $PtBr(BO)(PMe_3)_2$, were theoretically investigated with the density functional theory method. The BO^- ligand was quantitatively demonstrated to have extremely strong σ-donation but very weak d_π-electron-accepting abilities. Therefore, it exhibits a strong trans influence. The formation reaction occurs through a four-center transition state, in which the $B^{\delta+}$−$Br^{\delta-}$ polarization and the Br → Si and O p_π → B p_π charge-transfer interactions play key roles. The Gibbs activation energy ($\Delta G^{\circ\ddagger}$) and Gibbs reaction energy (ΔG°) of the formation reaction are 32.2 and −6.1 kcal/mol, respectively. The electron-donating bulky phosphine ligand is found to be favorable for lowering both $\Delta G^{\circ\ddagger}$ and ΔG°. In addition, the metal effect is examined with the nickel and palladium analogues and $MBrCl[BBr(OSiMe_3)](CO)(PR_3)_2$ (M = Ir and Rh). By a comparison of the $\Delta G^{\circ\ddagger}$ and ΔG° values, the M−BO (M = Ni, Pd, Ir, and Rh) bonding nature, and the interaction energy between $[MBrCl(CO)(PR_3)_2]^+$ and BO^- with those of the platinum system, $MBrCl(BO)(CO)(PR_3)_2$ (M = Ir and Rh) is predicted to be a good candidate for a stable oxoboryl complex.

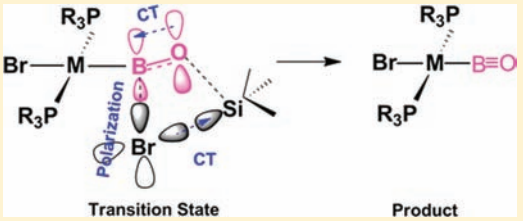

INTRODUCTION

In the last 2 decades, multiple-bonded compounds that involve one or two heavier main-group elements in the p block have attracted extensive interest.[1] One of the most important reasons is the challenge to the well-known double-bond rule that elements with a principal quantum number of larger than 2 cannot form a multiple bond either with themselves or with other elements.[2] Another reason is to find alternatives to versatile alkenes and alkynes, which would exhibit new interesting bonding nature, electronic structure, and molecular properties. In this regard, significant developments have been achieved by the syntheses of Si═Si double-bonded[3] and Si≡Si triple-bonded[4] compounds. Besides, many multiple-bonded systems containing group 15[5] and 16[6] heavier elements have also been synthesized.

Though many multiple-bonded compounds have been isolated between p-block first-row elements, as is well-known, the multiple-bonded compounds of boron elements have not been investigated well, as reviewed recently,[1,7] except for B═C double-bonded[8] and B≡N triple-bonded[9] compounds. For instance, a boron radical anion with a B═B double-bond character was experimentally detected in 1981 but was not isolated.[10] The reports of isolation and characterization of B═As and B═B double-bonded compounds were presented in 1990[11] and 1992,[12] respectively. In 1999, analogous tetraaminodiborate dianions were reported by Nöth et al.[13] Recently, neutral diborene compounds were reported by Robinson's group.[14] A theoretical study of an experimentally viable compound with a B═B double bond was carried out by Kaufmann and Schleyer's group.[15] The reports of the triple-bonded boron compounds have been much more limited. One neutral compound OCB≡BCO was detected under an argon matrix,[16] and its bonding nature was analyzed theoretically.[16,17] Also, synthesis of the B−O multiple-bonded compound has been very difficult for a long time. This is surprising because B≡N triple-bonded compounds were synthesized and well characterized.[9] One of the reasons is that the B−O bond is highly polarized and easily undergoes oligomerization reaction to form a B−O−B linkage rather than remaining as a B═O double or B≡O triple bond. In fact, the R−BO (R = alkyl) species including a B═O double bond was detected in the gas phase or a low-temperature argon matrix,[18] but it could not be isolated because it forms a dimer or trimer in solution.

In the past few years, however, new progress has been successfully made in the chemistry of the B−O multiple-bonded species. Cowley and co-workers successfully isolated a stable compound [β-diketiminate](BO) → $AlCl_3$.[19] In this species, the B−O bond is considered to be a double bond with a bond length of 1.304 Å. In 2010, more progress was achieved by Braunschweig et al.[20,21] They synthesized a remarkably stable neutral platinum(II) oxoboryl complex, $PtBr(BO)(PCy_3)_2$, as shown in eq 1. The short B−O distance (1.2103 Å) and large B−O stretching frequencies ν(B−O) (1853 and 1797 cm^{-1}) suggest that the BO moiety has a triple-bond feature. This was confirmed by the bond index calculation.[20]

In addition to the neutral platinum(II) oxoboryl complex, neutral platinum(II) iminoboryl complexes ($L_nMB{\equiv}NR$) were

Received: November 21, 2011
Published: March 29, 2012

   dx.doi.org/10.1021/ic202499u | Inorg. Chem. 2012, 51, 4597−4605

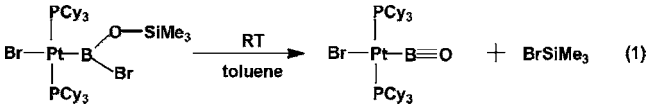

reported.[22] They were synthesized by a reaction similar to that of eq1; see eq 2.

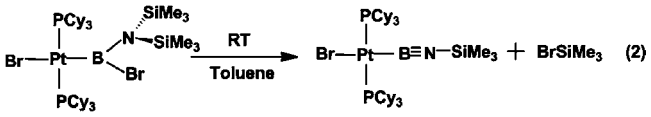

These new reactions are of considerable interest because the strong Si−O and Si−N bonds are broken and the B≡O and B≡N triple bonds are formed. However, the reaction mechanisms, electronic processes, geometry changes, and transition states of these reactions are not clear, to our knowledge. Such information is valuable and indispensable not only for the correct understanding of these reactions but also for further development of the chemistry of similar multiple-bonded compounds.

In the neutral oxoboryl complex $PtBr(BO)(PCy_3)_2$, the BO moiety is considered to be an anion.[23] The BO^- anion is an isoelectronic species of CO, where we use BO^- with a negative charge to describe this ligand when it is discussed as an independent moiety hereafter. Finding alternatives to CO is interesting in a wide area of chemistry. In this aspect, theoretical studies of transition-metal oxoboryl complexes have been reported by Baerends'[24] and Schaefer's groups.[25] However, there are important issues to be elucidated such as the trans influence of the BO^- ligand, the quantitative evaluation of σ-donation and π-back-donation interactions in the M−BO bond, and the theoretical prediction of new transition-metal oxoboryl complex.

In this work, we theoretically investigated the platinum(II) oxoboryl complex $PtBr(BO)(PR_3)_2$ (R = CF_3, Me, or *i*-Pr) and its formation reaction with density functional theory (DFT). Our purposes here are to clarify the differences in the coordination bonding nature and trans influence between the BO^- ligand and such well-known isoelectronic ligands as CO, CN^-, and NO^+, to disclose the reaction features of the formation reaction shown in eq 1, and to present a theoretical prediction on a candidate of a stable transition-metal oxoboryl complex.

COMPUTATIONAL DETAILS

Geometry optimizations were carried out with the DFT method using the B3LYP functional.[26,27] Two kinds of basis set systems, BS-I and BS-II, were used in this work. In BS-I, the effective core potentials (ECPs) of LANL2DZ[28] were employed for transition metals (Ni, Pd, Pt, Ir, and Rh) to replace their core electrons. Valence electrons of Pt and Ir were represented by (541/541/111/1),[28−30] those of Pd and Rh by (541/541/211/1),[28−30] and those of Ni by (541/541/311/1).[28−30] The 6-311+G* basis sets were used for Br and Cl atoms. For other atoms, the 6-311G* basis sets[31] were employed. In BS-II, core electrons of Ni, Pd, Pt, Ir, and Rh were replaced with Stuttgart−Dresden−Bonn ECPs,[32] and their valence electrons were represented with (311111/22111/411/11) basis sets.[32,33] For other atoms, the same basis sets as those of BS-I were used. BS-I was employed for geometry optimization and vibrational frequency calculation. The better basis set system, BS-II, was used for the evaluation of energy changes because the energy change is rather sensitive to the basis set.[34] All transition states were verified with intrinsic reaction coordinate (IRC) calculation.[35] The polarizable continuum model[36] was employed to compute the potential energy in the solvent (toluene), where gas-phase-optimized structures were employed. The Gibbs energy in solution was calculated in the same way as that described in our previous works,[37] in which the entropy of translational movement was evaluated with the method developed by Whitesides et al.[38] The scale factor for the vibrational frequency was not employed here. All of these calculations were carried out with the *Gaussian 09* program.[39] In this work, B3LYP computational results are employed for discussion after a careful check of the reliability; see the Supporting Information, p S3 and Table S1.

RESULTS AND DISCUSSION

In the first subsection, the Pt−BO bonding nature is discussed in comparison with the Pt−CO, Pt−CN, and Pt−NO bonds. In the next two subsections, the mechanism and electronic process of the formation reaction of the platinum(II) oxoboryl complex $PtBr(BO)(PMe_3)_2$ ($\mathbf{2}_{PtBO}$) are investigated. Then, the effects of the phosphine ligand and transition metal (M = Ni, Pd, Ir, and Rh) on the formation reaction are explored. In the last subsection, the theoretical prediction of a new candidate for a stable transition-metal oxoboryl complex is presented.

Pt−BO Bonding Nature and Its Comparison with the Pt−L (L = CO, CN^-, and NO^+) Bond. Optimized geometries of platinum(II) complexes with L = BO^-, CO, CN^-, and NO^+ are shown in Figure 1. The Pt−Br bond distance gradually

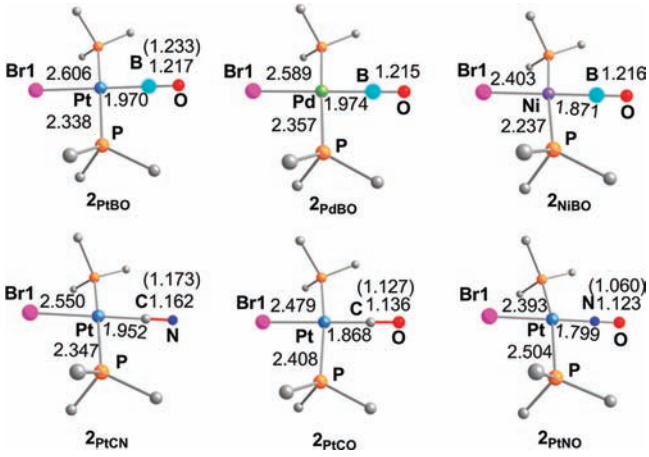

Figure 1. Optimized structures of $\mathbf{2}_{PtBO}$, $\mathbf{2}_{PtCN}$, $\mathbf{2}_{PtCO}$, $\mathbf{2}_{PtNO}$, $PdBr(BO)(PMe_3)_2$ ($\mathbf{2}_{PdBO}$), and $NiBr(BO)(PMe_3)_2$ ($\mathbf{2}_{NiBO}$). H atoms on the methyl groups are omitted for clarity. In parentheses are the bond distances of free L molecules. Distances are in angstroms.

decreases in the order $\mathbf{2}_{PtBO}$ (2.606 Å) > $PtBr(CN)(PMe_3)_2$ ($\mathbf{2}_{PtCN}$; 2.550 Å) > $[PtBr(CO)(PMe_3)_2]^+$ ($\mathbf{2}_{PtCO}$; 2.479 Å) > $[PtBr(NO)(PMe_3)_2]^{2+}$ ($\mathbf{2}_{PtNO}$; 2.393 Å), where the Pt−Br distance is in parentheses. This trend indicates that the trans influence of the L ligand becomes weaker in the order BO^- > CN^- > CO > NO^+. Interestingly, the B−O and C−N distances become moderately shorter by 0.016 and 0.011 Å, respectively, upon coordination with the Pt center, while the C−O and N−O distances become moderately longer by 0.009 and 0.063 Å, respectively. These results provide us with the following questions: (1) what differences exist in the bonding nature between Pt−BO and Pt−L (L = CO, CN^-, and NO^+), (2) why does the BO^- ligand have the strongest trans influence, and (3) why do the B−O and C−N bond distances become shorter but the C−O and N−O bond distances become longer in the transition-metal complexes than in the free diatomic molecules?

In general, the M−L bonding nature is discussed in terms of the σ donation from the ligand to the metal center and the π

dx.doi.org/10.1021/ic202499u | Inorg. Chem. 2012, 51, 4597−4605

Table 1. Important Molecular Orbitals and Their Electron Populations[a] of $[MBr(PMe_3)_2]^+$ and L Ligand in $MBrL(PMe_3)_2$ (L = BO^-, CN^-, CO, and NO^+)

		$[MBr(PMe_3)_2]^+$			L		
		LUMO	HOMO[b]	HOMO−3[c]	5σ	π^*_1	π^*_2
L	M	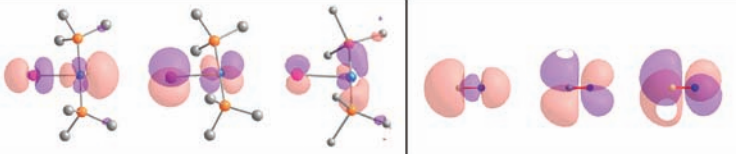					
BO^-	Pt	1.174 *e*	1.946 *e*	1.972 *e*	0.702 *e*	0.068 *e*	0.042 *e*
	Pd	1.076 *e*	1.975 *e*	1.981 *e*	0.853 *e*	0.055 *e*	0.034 *e*
	Ni	0.999 *e*	1.976 *e*	1.985 *e*	0.857 *e*	0.053 *e*	0.023 *e*
	Ir	1.212 *e*	1.977 *e*	1.973 *e*	0.596 *e*	0.043 *e*	0.035 *e*
	Rh	1.190 *e*	1.910 *e*	1.979 *e*	0.729 *e*	0.040 *e*	0.024 *e*
CN^-	Pt	0.608 *e*	1.961 *e*	1.975 *e*	1.481 *e*	0.067 *e*	0.057 *e*
CO	Pt	0.413 *e*	1.841 *e*	1.881 *e*	1.636 *e*	0.210 *e*	0.183 *e*
NO^+	Pt	0.179 *e*	1.497 *e*	1.564 *e*	1.860 *e*	0.479 *e*	0.530 *e*

[a]The electron population of each MO is presented here. In the LUMO, the population increases from zero to the number here in the complex. In the doubly occupied orbital (HOMO, HOMO−1, and 5σ), the population decreases from two to the number here in the complex. [b]HOMO−2 for Ni and Pd, HOMO−3 for Ir, and HOMO−4 for Rh systems. [c]HOMO for Ni and Pd, HOMO−4 for Ir, and HOMO−5 for Rh systems.

back-donation from the metal center to the ligand. To discuss those interactions, it is crucial to separately evaluate σ-donation and π-back-donation interactions. The natural bond orbital (NBO) population analysis cannot present such kind of information because the electron population provided by this method is a result of both σ donation and π back-donation. In general, the molecular orbital (MO) of a total system AB can be represented by a linear combination of MOs of fragments A and B; see eq 3,[40]

$$\varphi_i^{AB} = \sum_m C_{im}^A \varphi_m^A + \sum_n C_{in}^B \varphi_n^B \quad (3)$$

where φ_i^{AB} represents the *i*th MO of the complex AB and φ_m^A and φ_n^B are the *m*th and *n*th MOs of fragments A and B, respectively. C_{im}^A and C_{in}^B are expansion coefficients of φ_m^A and φ_n^B, respectively. The electron populations of φ_m^A and φ_n^B can be obtained from these coefficients, C_{im}^A and C_{in}^B. This idea was employed in the discussion of the contributions of σ-donation and π-back-donation interactions to the coordination bond in our previous works.[41] Here, the oxoboryl complex $\mathbf{2}_{PtBO}$ is divided into such two moieties as $[PtBr(PMe_3)_2]^+$ and BO^-.[42] The electron populations of important MOs of $[PtBr(PMe_3)_2]^+$ and BO^- are shown in Table 1 with MO pictures. The population on the lowest unoccupied molecular orbital (LUMO) of $[PtBr(PMe_3)_2]^+$ considerably increases to 1.174e, where the LUMO mainly consists of the Pt d_σ orbital. Consistent with this increase, the population on the lone-pair orbital (highest occupied molecular orbital HOMO) of BO^- considerably decreases to 0.702e. These results clearly indicate that charge transfer (CT) substantially occurs from the lone-pair orbital of BO^- to the d_σ orbital of the $[PtBr(PMe_3)_2]^+$ moiety. On the other hand, the populations of two π* orbitals of BO^- moderately increase to 0.068e and 0.042e, respectively. Consistent with these increases in the population, the electron populations on HOMO and HOMO−3 of the $[PtBr(PMe_3)_2]^+$ moiety moderately decrease by 0.074e and 0.028e, respectively, where HOMO and HOMO−3 mainly consist of the d_π orbital of Pt. These results demonstrate that the σ donation from BO^- to Pt is extremely strong and provides a predominant contribution to the Pt−BO bond. On the other hand, the π back-donation is very weak and its contribution to the Pt−BO bond is very small.

Comparison of the Pt−BO bond with other Pt−L bonds (L = CN^-, CO, and NO^+) is interesting. As shown in Table 1, the electron population on the LUMO of the $[PtBr(PMe_3)_2]^+$ moiety considerably increases in the order NO^+ < CO < CN^- ≪ BO^-. Consistent with this result, the electron population on the HOMO (the lone pair orbital) of BO^-, CN^-, CO, and NO^+ decreases in the order NO^+ > CO > CN^- ≫ BO^-. On the other hand, the electron populations on the π* orbitals increase in the order BO^- < CN^- < CO ≪ NO^+. These results indicate that the σ-donation becomes weaker in the order BO^- ≫ CN^- > CO > NO^+, but the d_π-electron-accepting ability becomes stronger in the reverse order.

The above results provide us with a clear explanation for the reason why BO^- has the strongest trans influence. The LUMO of $[PtBr(PMe_3)_2]^+$ contains an antibonding overlap between the p_σ orbital of Br and the d_σ orbital of Pt, while the HOMO of $[PtBr(PMe_3)_2]^+$ contains a d_π−p_π antibonding overlap between Pt and Br, as shown in Table 1. Thus, σ-donation of the L ligand, which supplies the electron population to the LUMO of the Pt moiety, induces weakening of the Pt−Br bond. On the other hand, π back-donation from the Pt moiety to L reduces the electron population on the HOMO of $[PtBr(PMe_3)_2]^+$, which leads to strengthening of the Pt−Br bond. Because the BO^- ligand has the strongest σ-donation and the weakest d_π-electron-accepting abilities in these ligands, as discussed above, it exhibits the strongest trans influence. The weakest trans influence of the NO^+ ligand and the decreasing order of the trans influence, BO^- ≫ CN^- > CO > NO^+, can be understood in a similar way.

dx.doi.org/10.1021/ic202499u | Inorg. Chem. 2012, 51, 4597−4605

It is interesting to discuss the reason why the B−O and C−N distances become shorter but the C−O and N−O distances become longer in their platinum(II) complexes than in free diatomic molecules. Previous theoretical studies of several CO complexes disclosed that the electrostatic effect of the cation moiety induces polarization of the bond orbital of the CO moiety, which leads to shortening of the C−O bond distance.[43] The same effect is orbserved here for BO^-, CN^-, and NO^+; see Figure S4 in the Supporting Infromation. On the other hand, the π back-donation of the metal moiety to the L ligand induces significant elongation of the interatomic distance of the L ligand. The π back-donation of the Pt moiety to the L ligand increases in the order L = BO^- (0.110e) < CN^- (0.124e) < CO (0.393e) ≪ NO^+ (1.009e), where in parentheses is the sum of the electron populations of the two π^* orbitals of the L ligand. In other words, bond elongation by π back-donation is larger than bond shortening by the electrostatic interaction in CO and NO^+ but less in BO^- and CN^-. These are the reasons why the B−O and C−N distances become shorter but the C−O and N−O distances become longer.

In summary, our computations quantitatively demonstrated that the BO^- ligand has extremely strong σ donation but very weak d_π-electron-accepting abilities. The next is CN^- and then CO, and the last is NO^+. This is the origin for the increasing order of the trans influence: NO^+ < CO < CN^- ≪ BO^-. The relationship between the σ donation ability of the ligand and its trans influence is clearly understood by the LUMO feature of the $[PtBr(PMe_3)_2]^+$ moiety.

Formation Reaction of Platinum(II) Oxoboryl Complex 2_{PtBO}; Geometry and Energy Changes. Optimized geometries of all species along the formation reaction are shown in Figure 2. In the reactant $PtBr[BBr(OSiMe_3)](PMe_3)_2$ ($\mathbf{1}_{PtMe}$), the B−O bond length is 1.335 Å. When going from $\mathbf{1}_{PtMe}$ to the transition state $\mathbf{TS}_{PtMe}$, the Pt−B and B−O distances become somewhat shorter by 0.064 and 0.081 Å, respectively, whereas the Pt−B−O angle considerably increases from 129° to 167°. On the other hand, the B−Br2 and Si−O bonds are considerably elongated by 0.718 and 0.267 Å, respectively; see Figure 2 for Br1 and Br2. Simultaneously, the Br2 and Si atoms are approaching each other. In $\mathbf{TS}_{PtMe}$, the Br2···Si distance (2.754 Å) is about 20% longer than that (2.285 Å) in the byproduct $BrSiMe_3$, suggesting that the Br−Si bond is not formed completely, but some bonding interaction is already formed. The Gibbs activation energy ($\Delta G^{\circ\ddagger}$) of this reaction is 32.3 kcal/mol. When going from $\mathbf{TS}_{PtMe}$ to the product $\mathbf{2}_{PtBO}$, the B−O distance becomes further shorter by 0.037 Å. Interestingly, the Pt−Br1 distance in $\mathbf{2}_{PtBO}$ (2.606 Å) is shorter than that in $\mathbf{1}_{PtMe}$ (2.670 Å) despite the shorter Pt−B distance in $\mathbf{2}_{PtBO}$ than that in $\mathbf{1}_{PtMe}$. This result suggests that the boryl $[BBr(OSiMe_3)]^-$ ligand exhibits a stronger trans influence than the oxoboryl BO^- ligand. This is because the lone-pair orbital of the boryl ligand lies at much higher energy (1.47 eV) than that of the oxoboryl ligand (0.80 eV), where the Kohn−Sham orbital energy is presented. For the whole reaction, the Gibbs reaction energy (ΔG°) is −6.1 kcal/mol and the reaction enthalpy change (ΔH°) is 4.9 kcal/mol (Table 3), indicating that the reaction is endothermic and the increase of the entropy is important for the negative ΔG° value; remember that two species are produced from one compound in this reaction.

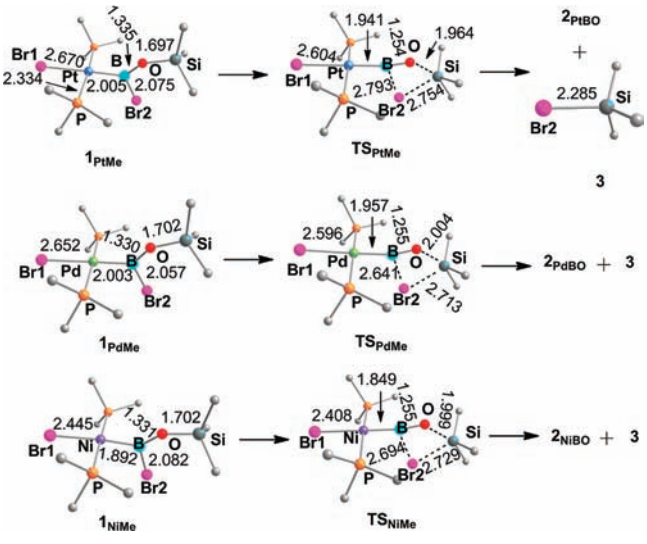

Figure 2. Optimized structures of the reactant and transition state (TS) in the formation reaction of the oxoboryl complex $MBr(BO)(PMe_3)_2$ from $MBr[BBr(OSiMe_3)](PMe_3)_2$ (M = Pt, Pd, and Ni). H atoms in the PMe_3 and $SiMe_3$ groups are omitted for clarity. All of the distances are in angstroms.

In addition, the structural parameters along the reaction pathway were investigated by the IRC calculation. Upon going from the reactant to the product, the B−Br2 distance gradually increases, as shown in Figure 3A, while the Br2···Si distance gradually decreases. It is noted that the Si−O distance changes little in the very early stage of the reaction. Then, it is moderately elongated around the transition state and substantially in the late stage of the reaction. On the other hand, B−Br2 bond elongation occurs earier than Si−O bond elongation, which is considerably elongated around the transition state. These results suggest that Si−O bond elongation does not easily occur and that the reaction is induced by B−Br2 bond elongation.

Electronic Processes of the Formation Reaction of the Platinum(II) Oxoboryl Complex 2_{PtBO}. The NBO population changes along the reaction coordinate are presented in Figure 3B. In the early stage of the reaction (stage a in Figure 3B), the Br2 atomic population considerably increases, but the B atomic population considerably decreases. On the other hand, the O atomic population slightly decreases and the Si atomic population changes little. This is consistent with the slight elongation of the Si−O bond in this reaction stage. Around the reaction stage b, the Br2 atomic population increases to almost the same extent as the sum of both O and B atomic populations decreases; see Figure 3B. These population changes indicate that B−Br2 bond elongation induces $B^{\delta+}$−$Br2^{\delta-}$ polarization to decrease the B atomic population in this stage. Hence, CT from the O atom to the B atom occurs to compensate for the decrease in the B atomic population, leading to a slight shortening of the B−O distance.

Around TS_{PtMe}, B−Br2 elongation further occurs, which strengthens $B^{\delta+}$−$Br2^{\delta-}$ polarization. However, the Br2 atomic population begins to decrease rapidly in this reaction stage and the Si atomic population increases steeply, as presented in Figure 3B. These population changes indicate that CT starts to occur from Br2 to Si. Actually, the Br p_π orbital is found in the occupied level and the Si p orbital in the unoccupied level in TS_{PtMe}, as displayed in Figure 4. These orbitals participate in CT from Br2 to Si. It is noted that the O atomic population starts to significantly decrease. Si−O elongation further occurs here, which weakens the participation of the O p orbital in the

dx.doi.org/10.1021/ic202499u | Inorg. Chem. 2012, 51, 4597−4605

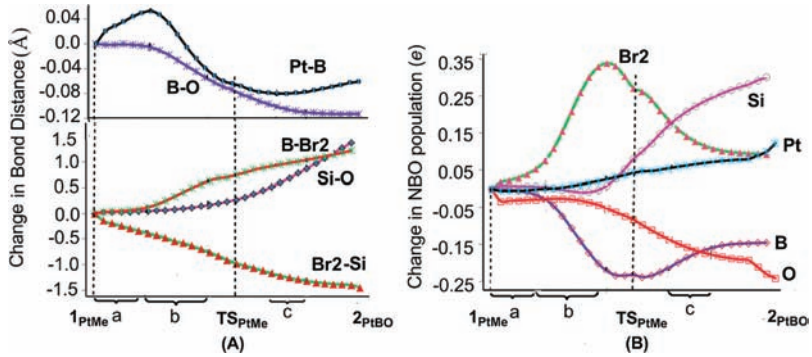

Figure 3. Changes in several important bond distances and electron populations along the IRC of the formation reaction of $\mathbf{2}_{PtBO}$. A positive value represents an increase in the population or bond distance relative to those in the reactant $\mathbf{1}_{PtMe}$ and vice versa. The DFT/BS-II level was employed.

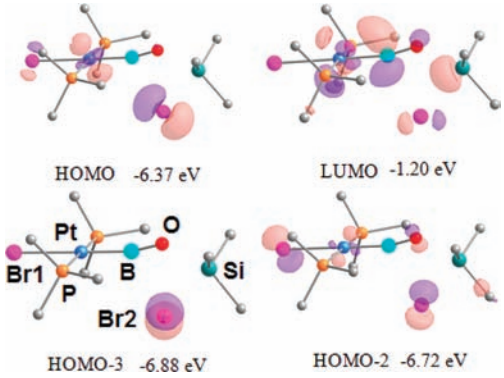

Figure 4. Several important occupied orbitals localized on the Br2 atom and a vacant orbital localized on the silyl moiety in $\mathbf{TS}_{PtMe}$.

Si−O bond. As a result, CT from the O p orbital to the B p orbital becomes stronger around TS_{PtMe}, leading to a further shortening of the B−O bond; see Scheme 1 for these CTs.

Scheme 1

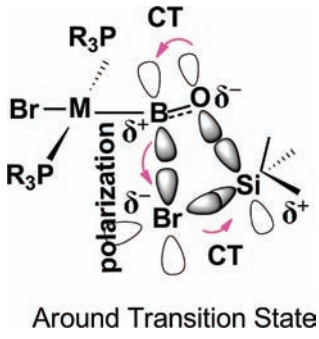

In the later stage c (see Figure 3), the Br2 atomic population further decreases and the Si atomic population further increases, indicating that CT from Br2 to Si becomes stronger. The Br2−Si distance continues to decrease, as displayed in Figure 3A. These structural and electron population changes are consistent with the Br2−Si bond formation in this reaction. Another important change is that the B atomic population increases to almost the same extent as that of the O atomic population decreases in stage c, indicating that the important change in the BO moiety is the strengthening of CT from the O p_π orbital to the B p_π orbital. This CT participates in the formation of a new π-bonding interaction between the B and O atoms, which corresponds to the conversion of the B═O double bond to the B≡O triple bond.

Phosphine Ligand Effect on the Formation Reaction. As listed in Table 3, the $\Delta G^{\circ\ddagger}$ and ΔG° are 41.7 and 3.8 kcal/mol, respectively, for the formation reaction of $PtBr(BO)[P(CF_3)_3]_2$, 32.3 and −6.1 kcal/mol for that of $\mathbf{2}_{PtBO}$, and 24.8 and −14.7 kcal/mol for that of $PtBr(BO)[P(i\text{-}Pr)_3]_2$. Apparently, the electron-donating bulky phosphine is favorable for the formation reaction of the oxoboryl complex. As discussed above, the boryl $[BBr(OSiMe_3)]^-$ ligand is more electron-donating than the oxoboryl BO^- ligand. Hence, the electron-donating phosphine much more destabilizes the boryl reactant $PtBr[BBr(OSiMe_3)](PR_3)_2$ than the oxoboryl product $PtBr(BO)(PR_3)_2$. In addition, the boryl reactant is more congested than the oxoboryl product. From the steric viewpoint, therefore, the bulky phosphine ligand is more unfavorable for the reactant than for the product. Because of these two factors, the formation reaction becomes more exothermic by the electron-donating bulky phosphine system.

Also, the electron-donating phosphine stabilizes the transition state from two aspects. In one aspect, it is in favor of the $B^{\delta+}-Br2^{\delta-}$ polarization, the accumulation of the electron population on the Br2 atom, and the Br2 → Si CT interaction, as follows: Because CT from the $[BBr(OSiMe_3)]^-$ moiety to Pt reduces the B atomic population, this CT suppresses $B^{\delta+}-Br2^{\delta-}$ polarization, which is unfavorable for the accumulation of the electron population on the Br2 atom. The electron-donating phosphine can suppress this CT, and hence it is favorable for $B^{\delta+}-Br2^{\delta-}$ polarization and the accumulation of the electron population on the Br2 atom. In fact, the negative charge on Br2 increases in the order $P(CF_3)_3$ (−0.30e) < PMe_3 (−0.56e) < $P(i\text{-}Pr)_3$ (−0.60e) at the transition state, as shown in Table 2. As a result, the Br2 → Si CT interaction becomes stronger in the order $P(CF_3)_3$ < PMe_3 < $P(i\text{-}Pr)_3$. Another is the Pt−B bond strengthening in the transition state. As discussed above, the Pt−B bond strengthening in the transition state arises from $d_\pi-p_\pi$ back-donation from Pt to B. The electron-donating phosphine enhances this $d_\pi-p_\pi$ back-donation, which induces considerable shortening of the Pt−B bond. In fact, the extent of Pt−B bond shortening increases in the order $P(CF_3)_3$ (0.040 Å) < $P(i\text{-}Pr)_3$ (0.063 Å) ∼ PMe_3 (0.064 Å), where the extent of the Pt−B bond shortening is in parentheses.

In summary, the formation reaction occurs through $B^{\delta+}-Br2^{\delta-}$ polarization and Br2 → Si and O p_π → B p_π CT interactions. The electron-donating bulky phosphine is favorable for the reaction through (1) the enhancement of

dx.doi.org/10.1021/ic202499u | Inorg. Chem. 2012, 51, 4597−4605

Table 2. Ligand Effects on the Interaction Energy between BO^- and the Metal Moiety, Several Important Geometrical Parameters, and NBO Population in 2_{PtBO}

	PR_3		
	$P(CF_3)_3$	PMe_3	$P(i\text{-}Pr)_3$
Pt–BO interaction energy[a] (kcal/mol unit)	158.6	154.7	138.5
R(Pt–P) (Å)	2.302	2.339	2.394
R(Pt–B) (Å)	2.001	1.970	1.958
R(Pt–Br1) (Å)	2.567	2.606	2.635
Population (in e Units)[b]			
Pt	−0.58	−0.61	−0.49
d	9.18	9.21	9.23
s	0.71	0.78	0.70
p	0.67	0.61	0.53
BO	−0.04	−0.09	−0.14
Br1	−0.37	−0.50	−0.52
PR_3	0.49	0.60	0.57

[a]See ref 45. [b]NBO charge for atom (or group) and population for the s, p, and d orbitals.

$B^{\delta+}$–$Br2^{\delta-}$ polarization and electron accumulation on Br2, (2) the enhancement of back-donation from Pt to B in the transition state, and (3) destabilization of the boryl complex (reactant) more than the oxoboryl complex (product) through both electronic and steric effects.

Formation Reactions of Oxoboryl Complexes of Other Transition-Metal Systems and Theoretical Prediction of the New Oxoboryl Complex. The formation reaction of a oxoboryl complex is explored in such systems as nickel and palladium analogues, IrBrCl[BBr(OSiMe$_3$)](CO)-(PMe$_3$)$_2$,[44] and its rhodium analogue here. As shown in Figure 2, the geometry changes in the palladium and nickel reaction systems are almost the same as those of the platinum reaction system. The $\Delta G^{\circ\ddagger}$ and ΔG° values are 35.5 and −5.9 kcal/mol, respectively, for nickel and 34.5 and −4.5 kcal/mol for palladium, as shown in Table 3, indicating that the formation reaction is difficult in nickel and palladium systems. Although there is no big difference in the B, O, Si, and Br2 atomic populations among these complexes, as demonstrated in Tables 4 and 4 and 5, we found that the extent of M–B bond shortening in the transition state becomes larger in the order Ni

Table 3. Gibbs Activation Energy ($\Delta G^{\circ\ddagger}$)[a], Gibbs Reaction Energy (ΔG°)[b], and Enthalpy Change (ΔH°)[c] for the Formation Reaction of the Oxoboryl Complex $MBr(BO)(PR_3)_2$ (kcal/mol)

M	PR_3	$\Delta G^{\circ\ddagger}$	ΔG°	ΔH°
	$P(CF_3)_3$	41.7	3.8	15.6
Pt	PMe_3	32.3	−6.1	4.9
	$P(i\text{-}Pr)_3$	24.8	−14.7	−2.8
Ni	PMe_3	35.5	−5.9	5.2
Pd	PMe_3	34.6	−4.5	6.6
Ir	PMe_3	31.3	−7.5	4.3
	$P(i\text{-}Pr)_3$	25.3	−13.8	−1.80
Rh	PMe_3	32.6	−6.4	5.0
	$P(i\text{-}Pr)_3$	25.6	−13.4	−1.43

[a]The Gibbs energy difference between the transition state and the precursor complex. [b]The Gibbs energy difference between the reactant and the sum of the products. [c]The enthalpy change between the reactant and the sum of the products.

Table 4. Changes[a] of Electron Populations in the Formation Reaction of 2_{PtBO}

			Products	
	1_{PtMe}	TS_{PtMe}	2_{PtBO}	$BrSiMe_3$
Pt	78.48	78.52	78.61	
d	9.23	9.22	9.21	
s	0.73	0.71	0.78	
p	0.51	0.59	0.61	
B(Br2)(OSiMe$_3$)[b]	−0.10	−0.21		
B	0.64	0.90	0.78	
O	−1.11	−1.1	−0.87	
$SiMe_3$	0.66	0.50		0.38
Br2[b]	−0.29	−0.57		−0.38
PMe_3	0.57	0.61	0.60	
Br1[b]	−0.56	−0.49	−0.50	

[a]A positive value represents increase in electron population and *vice versa*. [b]See Figure 2 for Br1 and Br2.

(0.043 Å) ~ Pd (0.046 Å) < Pt (0.064 Å). In accordance with this trend, π back-donation from the metal center to the boryl ligand increases in the order Ni (0.08e) ~ Pd (0.09e) < Pt (0.12e) in the transition state, where in parentheses is the sum of the electron populations on the π^* orbitals of the boryl group calculated by eq 3. Because π back-donation stabilizes the transition state, as discussed above, the platinum system is more reactive than the palladium and nickel systems.

In the iridium and rhodium systems, the Br and Cl ligands coordinate with the metal center at the positions cis and trans to the boryl ligand, respectively; see Figure 5. In the transition state, the Si–O and Si–Br2 distances and the Br2 and Si atomic populations are similar to those of the platinum system, as listed in Table 5. However, the B–Br2 bond distance is 3.085 Å in TS_{IrMe} and 3.019 Å in TS_{RhMe}, which are much longer than that in TS_{PtMe}. To compensate for the considerably long B–Br2 bond distance, M–B bond shortening is much larger in TS_{IrMe} (0.095 Å) and TS_{RhMe} (0.080 Å) than in TS_{PtMe}, which contributes to the stabilization of the transition states in the iridium and rhodium systems. As a result, the $\Delta G^{\circ\ddagger}$ and ΔG° values for the iridium and rhodium systems are similar to those of the platinum system, as shown in Table 3. It is noted that the use of $P(i\text{-}Pr)_3$ considerably decreases both $\Delta G^{\circ\ddagger}$ and ΔG°; see Table 3 for $\Delta G^{\circ\ddagger}$ and ΔG° and Figure S3 in the Supporting Information for the geometry changes by the reaction. They are 25.3 and −13.8 kcal/mol, respectively, for the iridium system and 25.6 and −13.4 kcal/mol for the rhodium system. These values are similar to those of the platinum system, indicating that the formation reaction can occur in the iridium and rhodium systems similarly to the platinum system.

In addition, we examined the M–BO (M = Ir and Rh) bonding nature and the interaction energy between the metal moiety and the BO^- ligand. σ-donation of the BO^- ligand to the metal center decreases the electron population of the lone-pair orbital by 1.212e and 1.190e in 2_{IrMe} and 2_{RhMe}, respectively, indicating that σ donation is somewhat larger than that in the platinum system. π back-donation from the metal center to the BO^- ligand is slightly weaker than that in the platinum system because the sums of the π^*-orbital populations of BO^- is 0.097e, 0.064e, and 0.110e in 2_{IrMe}, 2_{RhMe}, and 2_{PtMe}, respectively. The Ir–BO and Rh–BO bond energies are 154.7 and 149.1 kcal/mol, respectively.

dx.doi.org/10.1021/ic202499u | Inorg. Chem. 2012, 51, 4597–4605

Table 5. NBO Population Changes[a] upon Going to the Transition State from the Reactant of the Formation Reaction of $MBr(BO)(PR_3)_2$ (M = Pt, Pd, or Ni) and $MBrCl(BO)(CO)(PR_3)_2$ (M = Ir or Rh)

	M = Pt			R = Me			
	R = CF_3	R = Me	R = *i*−Pr	M = Pd	M = Ni	M = Ir	M = Rh
M	−0.48	−0.53	−0.41	−0.41	−0.47	−1.33	−1.30
B	0.71	0.88	0.87	0.90	0.90	1.09	1.14
O	−0.98	−1.03	−0.98	−1.08	−1.10	−1.04	−1.05
Si	1.76	1.78	1.74	1.77	1.78	1.78	1.84
Br2[b]	−0.30	−0.57	−0.61	−0.56	−0.56	−0.56	−0.55
PR_3	0.47	0.63	0.60	0.59	0.61	0.82	0.75
boryl	−0.06	−0.22	−0.27	−0.23	−0.25	0.00	0.15
Br1[b]	−0.40	−0.49	−0.50	−0.52	−0.49	−0.27	−0.26
Δd_{M-B} (Å)[c]	−0.040	−0.064	−0.064	−0.046	−0.043	−0.095	−0.080

[a]A positive value represents an increase in the population upon going from the reactant to the transition state. [b]See Figure 2 for Br1 and Br2. [c]The difference in the M−B distance between the transition state and the reactant. A negative value represents the shortening of the M−B bond.

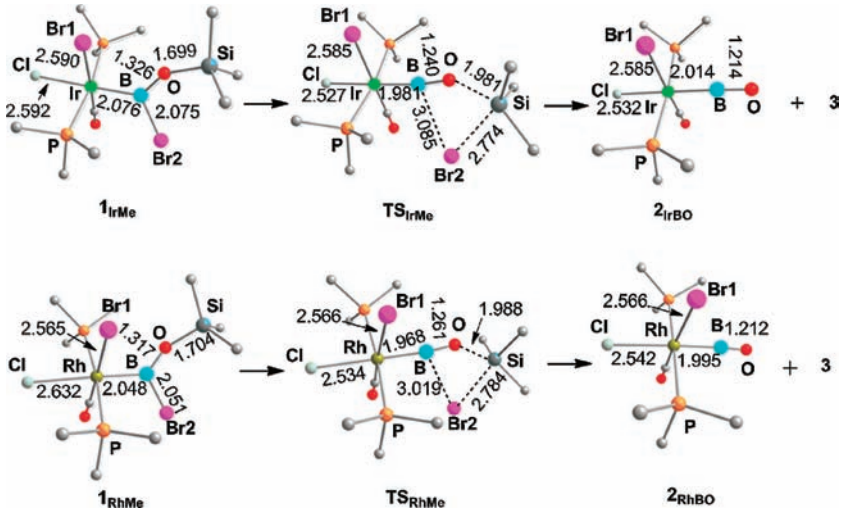

Figure 5. Optimized structures of the reactant, transition state (TS), and product in the formation reaction of $MBrCl(BO)(CO)(PMe_3)_2$ (M = Ir and Rh). H atoms on PMe_3 and $SiMe_3$ groups are omitted for clarity. All distances are in angstroms.

Here, we present the theoretical prediction on a promising candidate for a stable transition-metal oxoboryl complex based on three aspects. (1) The $\Delta G^{\circ\ddagger}$ and ΔG° values: The values of the rhodium and iridium systems are similar to those of the platinum system, but those of the palladium and nickel systems are somewhat larger; see Table 3. (2) The M−BO bonding nature: σ donation of the BO^- ligand to the metal center is somewhat stronger in the iridium and rhodium systems than in the platinum system, while π back-donations from the Ir and Rh centers to the BO^- ligand are slightly weaker than that from the Pt center. (3) The interaction energy between $[MBrCl(CO)(PMe_3)_2]^+$ and BO^-:[45] The interaction energy is evaluated to be 154.7, 149.1, 141.7, 130.9, and 123.6 kcal/mol for the Pt−BO, Ir−BO, Rh−BO, Pd−BO, and Ni−BO bonds, respectively. The Ir−BO bond moderately and the Rh−BO bond are somewhat weaker than the Pt−BO bond, while the Pd−BO and Ni−BO bonds are much weaker. According to the above three factors, the iridium and rhodium systems are close to the platinum system. The palladium and nickel systems are much worse than the platinum system. Taking all of these factors into consideration, it is predicted that $MBrCl(BO)(CO)(PR_3)_2$ (M = Ir and Rh) is a good candidate for a stable oxoboryl complex, similar to $PtBr(BO)(PR_3)_2$.

CONCLUSIONS

In this theoretical work, we investigated the Pt−BO bonding nature, made its comparison with other Pt−L (L = CN^-, CO, and NO^+) bonds, and presented the mechanistic and electronic insights into the formation reaction of the oxoboryl complex $PtBr(BO)(PR_3)_2$ as well as the effects of the phosphine ligand and transition metal on this reaction. On the basis of the computational results, the following conclusions are presented:

(1) The BO^- ligand has extremely strong σ donation but very weak d_π-electron-accepting abilities. As a consequence, it exhibits a very strong trans influence.

(2) The formation reaction of the oxoboryl complex $\mathbf{2_{PtBO}}$ occurs through a four-center transition state, in which $B^{\delta+}$−$Br2^{\delta-}$ polarization and Br2 → Si and O p_π → B p_π CT interactions play key roles. The electron-donating bulky phosphine ligand is favorable for the reaction by enhancing $B^{\delta+}$−$Br2^{\delta-}$ polarization, stabilizing the transition state, and destabilizing the boryl complex (reactant) more than the oxoboryl complex (product).

(3) $MBrCl(BO)(CO)(PR_3)_2$ (M = Ir and Rh) is predicted to be a good candidate of a stable oxoboryl complex based on the comparisons in the $\Delta G^{\circ\ddagger}$ and ΔG° values of the formation reaction, the M−BO bonding nature, and the M−BO interaction energy between $MBrCl(BO)(CO)(PR_3)_2$ and $PtBr(BO)(PR_3)_2$.

dx.doi.org/10.1021/ic202499u | Inorg. Chem. 2012, 51, 4597−4605

■ ASSOCIATED CONTENT

Supporting Information

Complete representation of ref 39, discussion of the reliability of the B3LYP functional in this study, optimized structure of $\mathbf{2}_{PtBO}$ and the B−O frequency, geometry changes in the oxidative addition of $BBr_2(OSiMe_3)$ to $IrCl(CO)(PMe_3)_2$, geometry changes in the formation reaction of $MBrCl(BO)(CO)([P(i\text{-}Pr)_3]_2$ from $MBrCl[BBr(OSiMe_3)](CO)([P(i\text{-}Pr)_3]_2$, the B−O, C−N, C−O, and N−O distance changes by proton and one positive charge, geometry changes in the formation reaction of the $P(CF_3)_3$ and $P(i\text{-}Pr)_3$ complexes of platinum, electronic energies of $[PtBr(PMe_3)_2]^+$, BO^-, $[PtBr(PMe_3)_2]^+$, and BO^-, and potential energies both in the gas phase and in the solvent, zero-point energy, Gibbs free energies in the gas phase of all stationary points located in this work, and the M06L-calculated energy changes. This material is available free of charge via the Internet at http://pubs.acs.org.

■ AUTHOR INFORMATION

Corresponding Author

*E-mail: sakaki@moleng.kyoto-u.ac.jp.

Notes

The authors declare no competing financial interest.

■ ACKNOWLEDGMENTS

This work is financially supported by the Grants-in-Aid from Ministry of Education, Culture, Science, Sport, and Technology through Grants-in-Aid of Specially Promoted Science and Technology (No. 22000009) and Grand Challenge Project (IMS, Okazaki, Japan). We are also thankful to the computational facility at the Institute of Molecular Science, Okazaki, Japan.

■ REFERENCES

(1) Fischer, R. C.; Power, P. P. *Chem. Rev.* **2010**, *110*, 3877 and references therein.

(2) (a) Jutzi, P. *Angew. Chem., Int. Ed. Engl.* **1975**, *14*, 232. (b) Guseln'ikov, L. E.; Nametkin, N. S. *Chem. Rev.* **1979**, *79*, 529. (c) Kuchta, M. C.; Parkin, G. *Coord. Chem. Rev.* **1998**, *176*, 323. (d) Norman, N. C. *Polyhedron* **1993**, *12*, 2431.

(3) West, R.; Fink, M. J.; Michl, J. *Science* **1981**, *214*, 1343.

(4) Sekiguchi, A.; Kinjo, R.; Ichinohe, M. *Science* **2004**, *105*, 1755.

(5) (a) Yoshifuji, M.; Shima, I.; Inamoto, N.; Hirotsu, K.; Higuchi, T. *J. Am. Chem. Soc.* **1981**, *103*, 4587. (b) Tokitoh, N.; Arai, Y.; Okazaki, R.; Nagase, S. *Science* **1997**, *277*, 78. (c) Tokitoh, N.; Arai, Y; Sasamori, T.; Okazaki, R.; Shigeru Nagase, S.; Uekusa, H.; Ohashi, Y. *J. Am. Chem. Soc.* **1998**, *120*, 433. (d) Cowley, A. H.; Lash, J. G.; Norman, N. C.; Pakulski, M. *J. Am. Chem. Soc.* **1983**, *105*, 5506.

(6) (a) Pohl, S.; Niecke, E.; Krebs, B. *Angew. Chem., Int. Ed. Engl.* **1975**, *14*, 261. (b) Seppelt, K. *Angew. Chem., Int. Ed. Engl.* **1991**, *30*, 361. (c) Fleischer, R.; Stalke, D. *Coord. Chem. Rev.* **1998**, *176*, 431 and references cited therein.

(7) Scheschkewitz, D. *Angew. Chem., Int. Ed.* **2008**, *47*, 1995.

(8) Reviews: (a) Eisch, J. J. *Adv. Organomet. Chem.* **1996**, *39*, 355. (b) Berndt, A. *Angew. Chem., Int. Ed. Engl.* **1993**, *32*, 985.

(9) (a) Niedenzu, K.; Dawson, J. W. *Boron−Nitrogen Compounds*; Springer: Berlin, 1965. (b) Paetzold, P. *Adv. Inorg. Chem.* **1987**, *31*, 123. (c) Nöth, H. *Angew. Chem., Int. Ed. Engl.* **1988**, *27*, 1603.

(10) Berndt, A.; Klusik, H. *Angew. Chem., Int. Ed. Engl.* **1981**, *20*, 870.

(11) Petrie, M. A.; Shoner, S. C.; Dias, H. V. R.; Power, P. P. *Angew. Chem., Int. Ed. Engl.* **1990**, *29*, 1033.

(12) (a) Moezzi, A.; Bartlett, R. A.; Power, P. P. *Angew. Chem., Int. Ed. Engl.* **1992**, *31*, 8. (b) Moezzi, A.; Olmstead, M. M.; Power, P. P. *J. Am. Chem. Soc.* **1992**, *114*, 2715. (c) Power, P. P. *Inorg. Chim. Acta* **1992**, *198−200*, 443.

(13) Nöth, H.; Knizek, J.; Ponikwar, W. *Eur. J. Inorg. Chem.* **1999**, 1931.

(14) Wang, Y.; Quillian, B.; Wei, P.; Wannere, C. S.; Xie, Y.; King, R. B.; Schaefer, H. F. III; Schleyer, P. v. R.; Robinson, G. H. *J. Am. Chem. Soc.* **2007**, *129*, 12412.

(15) Kaufmann, E.; Schleyer, P. v. R. *Inorg. Chem.* **1988**, *27*, 3987.

(16) Zhou, M.; Tsumori, N.; Li, Z.; Fan, K.; Andrews, L.; Xu, Q. *J. Am. Chem. Soc.* **2002**, *124*, 12936.

(17) Ducati, L. C.; Takagi, N.; Frenking, G. *J. Phys. Chem. A* **2009**, *113*, 11693.

(18) Kinney, C. R.; Pontz, D. F. *J. Am. Chem. Soc.* **1936**, *58*, 197.

(19) Vidovic, D.; Moore, J. A.; Jones, J. N.; Cowley, A. H. *J. Am. Chem. Soc.* **2005**, *127*, 4566.

(20) Braunschweig, H.; Radacki, K.; Schneider, A. *Science* **2010**, *328*, 345.

(21) (a) Braunschweig, H.; Radacki, K.; Schneider, A. *Chem. Commun.* **2010**, *46*, 6473. (b) Braunschweig, H.; Radacki, K.; Schneider, A. *Angew. Chem., Int. Ed.* **2010**, *49*, 5993.

(22) (a) Braunschweig, H.; Radacki, K.; Rais, D.; Uttinger, K. *Angew. Chem., Int. Ed.* **2006**, *45*, 162. (b) Braunschweig, H.; Kupfer, T.; Radacki, K.; Schneider, A.; Seeler, F.; Uttinger, K.; Wu, H. *J. Am. Chem. Soc.* **2008**, *130*, 7974.

(23) $PtBr(BO)(PCy_3)_2$ is a four-coordinate planar complex, indicating that Pt takes the oxidation state of +2 and, hence, the BO moiety is considered to be an anion.

(24) Ehlers, A. W.; Baerends, E. J.; Bickelhaupt, F. M.; Radius, U. *Chem.—Eur. J.* **1998**, *4*, 210.

(25) Gong, X.; Li, Q.; Xie, Y.; King, R. B.; Schaefer, H. F. III. *Inorg. Chem.* **2010**, *49*, 10820.

(26) Becke, A. D. *J. Chem. Phys.* **1993**, *98*, 5648.

(27) (a) Becke, A. D. *Phys. Rev. A* **1988**, *A38*, 3098. (b) Lee, C.; Yang, W.; Parr, R. G. *Phys. Rev. B* **1988**, *37*, 785. (c) Miehlich, B.; Savin, A.; Stoll, H.; Preuss, H. *Chem. Phys. Lett.* **1989**, *157*, 200.

(28) Hay, P. J.; Wadt, W. R. *J. Chem. Phys.* **1985**, *82*, 299.

(29) Couty, M.; Hall, M. B. *J. Comput. Chem.* **1996**, *17*, 1359.

(30) Ehlers, A. W.; Böhme, D. S.; Gobbi, A.; Höllwarth, A.; Jonas, V.; Khler, K. F.; Stegmann, R.; Veldkamp, A.; Frenking, G. *Chem. Phys. Lett.* **1993**, *208*, 111.

(31) Krishnan, R.; Binkley, J. S.; Seeger, R.; Pople, J. A. *J. Chem. Phys.* **1980**, *72*, 650.

(32) Andrae, D.; Haeussermann, U.; Dolg, M.; Stoll, H.; Preuss, H. *Theor. Chim. Acta* **1990**, *77*, 123.

(33) Gonzalez, C.; Schlegel, H. B. *J. Chem. Phys.* **1989**, *90*, 2154.

(34) Tsukamoto, S.; Sakaki, S. *J. Phys. Chem. A* **2011**, *115*, 8520.

(35) (a) Fukui, K. *Acc. Chem. Res.* **1981**, *14*, 363. (b) Tomasi, J.; Persico, M. *Chem. Rev.* **1994**, *94*, 2027.

(36) Scalmani, G.; Frisch, M. J. *Abs. Pap. Am. Chem. Soc.* **2009**, *238*, 342.

(37) (a) Ishikawa, A.; Nakao, Y.; Sato, H.; Sakaki, S. *Inorg. Chem.* **2009**, *48*, 8154. (b) Zeng, G.; Sakaki, S. *Inorg. Chem.* **2011**, *50*, 5290. (c) Hashimoto, H.; Fukuda, T.; Tobita, H.; Ray, M.; Sakaki, S. *Angew. Chem., Int. Ed.* **2012**, in press.

(38) Mammen, M.; Shakhnovich, E. I.; Deutch, J. M.; Whitesides, G. M. *J. Org. Chem.* **1998**, *63*, 3821.

(39) Frisch, M. J.; et al. *Gaussian 09*, revision A.01; Gaussian, Inc.: Wallingford, CT, 2009.

(40) (a) Baba, H.; Suzuki, S.; Takemura, T. *J. Chem. Phys.* **1969**, *50*, 2078. (b) Kato, S.; Yamabe, S.; Fukui, K. *J. Chem. Phys.* **1974**, *60*, 572. (c) Dapprich, S.; Frenking, G. *J. Phys. Chem.* **1995**, *99*, 9352.

(41) (a) Ochi, N.; Nakao, Y.; Sato, H.; Sakaki, S. *J. Am. Chem. Soc.* **2007**, *129*, 8615. (b) Ochi, N.; Nakao, Y.; Sato, H.; Sakaki, S. *J. Phys. Chem. A* **2010**, *114*, 659. (c) Sakaba, H.; Oike, H.; Kawai, M.; Takami, M.; Kabuto, C.; Ray, M.; Nakao, Y.; Sato, H.; Sakaki, S. *Organometallics* **2011**, *30*, 4515.

(42) We also checked the possibility of reverse heterolytic bond rupture leading to $[PtBr(PMe_3)_2]^-$ and BO^+. However, the system $[PtBr(PMe_3)_2]^-$ + BO^+ is much more unstable than the system $[PtBr(PMe_3)_2]^+$ + BO^- by 162.6 kcal/mol in electronic energy. Hence,

we considered only the heterolytic rupture leading to $[PtBr(PMe_3)_2]^+$ and BO^-.

(43) (a) Goldman, A. S.; Krogh-Jespersen, K. *J. Am. Chem. Soc.* **1996**, *118*, 12159. (b) Lupinetti, A. J.; Fau, S.; Frenking, G.; Strauss, S. H. *J. Phys. Chem. A* **1997**, *101*, 9551.

(44) The oxidative addition of the B−Br σ bond of $BBr_2(OSiMe_3)$ to the Vaska-type complex $IrCl(CO)(PMe_3)_2$ is calculated to occur with $\Delta G^{\circ\ddagger}$ of 13.7 kcal/mol, indicating that $IrBrCl[BBr(OSiMe_3)](CO)(PMe_3)_2$ is a reasonable starting compound; see Figure S2 and Table S4 in the Supporting Information for details.

(45) The M−BO interaction energy = $E_{t[MBr(BO)(PMe_3)_2]} - E_{t[MBr(PMe_3)_2]^+} - E_{t[BO]^-}$, where we did not optimize separated species but assumed their geometries to be the same as those in the oxoboryl complex.

dx.doi.org/10.1021/ic202499u | *Inorg. Chem.* 2012, 51, 4597−4605